American Mineralogist, Volume 78, pages 980–987, 1993

The OH-F substitution in Ti-rich potassium richterite: Rietveld structure refinement and FTIR and micro-Raman spectroscopic studies of synthetic amphiboles in the system K_2O-Na_2O-CaO-MgO-SiO_2-TiO_2-H_2O-HF

GIANCARLO DELLA VENTURA*
Department of Geological Sciences, University of Manitoba, Winnipeg, Manitoba R3T 2N2, Canada
JEAN-LOUIS ROBERT, JEAN-MICHEL BÉNY
CRSCM-CNRS, 1A rue de la Férollerie, F-45071 Orléans Cedex 2, France
MATI RAUDSEPP, FRANK C. HAWTHORNE
Department of Geological Sciences, University of Manitoba, Winnipeg, Manitoba R3T 2N2, Canada

ABSTRACT

Amphiboles were synthesized along the join $K(NaCa)Mg_5(Si_{7.4}Ti_{0.6})O_{22}(OH,F)_2$ from (OH) = 2 to F = 2 apfu (atoms per formula unit). Rietveld structure refinement shows that Ti^{4+} is completely ordered at the T2 site. For the OH end-member starting composition, a single-phase amphibole is obtained with 0.6 apfu of Ti. Along the OH-F join, amphibole ± priderite ± titanite ± rutile is produced, and the Ti content of the amphibole decreases to 0.16 apfu in end-member fluor-richterite.

The infrared spectra in the principal OH-stretching region show a main band for the Ti-rich OH end-member centered at 3728 cm^{-1}. This band is assigned to a MgMgMg-OH → K configuration. When F is present, a new band appears at 3711 cm^{-1}; the position of this band remains constant while its intensity increases with increasing F content, suggesting that the OH-F substitution is not random. The Raman spectra in the region of 1200–30 cm^{-1} show bands assigned to vibrations of $Ti^{4+}O_4$ groups that decrease in intensity with decreasing Ti^{4+} in the amphibole.

The decrease in solubility of Ti in potassium richterite for increasing F content at O3 is compatible with the crystal-chemical model for $^{[4]}Ti^{4+} \rightleftharpoons Si$ substitution in richterite proposed by Oberti et al. (1992).

INTRODUCTION

Della Ventura and Robert (1988) showed, using infrared spectroscopy and X-ray powder diffraction, that Ti^{4+} enters the fourfold-coordinated sites in synthetic potassium richterite by direct substitution for Si. Additional techniques (XANES, Raman, EXAFS) have since been used to confirm the coordination of Ti^{4+} in these amphiboles (Mottana et al., 1990; Della Ventura et al., 1991; Paris et al., 1993). Oberti et al. (1992) have shown that $^{[4]}Ti^{4+}$ does occur in these amphiboles and that $^{[4]}Ti$ is strongly ordered at the T2 site.

The solubility of Ti in synthetic potassium richterite is strongly temperature dependent (Della Ventura et al., 1991); in agreement with the findings of Wagner and Velde (1986), Thy et al. (1987), and Oberti et al. (1992) for natural amphiboles. Most Ti-rich richterite contains appreciable Fe and F, but the effect of these two elements on the stability of Ti-rich amphiboles has not been characterized. The present study was undertaken in order to fill this gap. This paper reports the results obtained for synthetic amphibole compositions along the join $K(NaCa)Mg_5[Si_{7.4}Ti_{0.6}]O_{22}(OH)_2$-$K(NaCa)Mg_5[Si_{7.4}Ti_{0.6}]O_{22}(F)_2$ (defined as $RTi_{0.6}$ – $FRTi_{0.6}$ throughout the following text).

EXPERIMENTAL METHODS

Synthesis

Experiments at T = 900 °C, P_{H_2O} = 1 kbar, were done in internally heated vessels; experiments at 800 °C, 1 kbar, were done in externally heated vessels. Starting materials were prepared as silicate gels, according to the method of Hamilton and Henderson (1968). Ti in stoichiometric proportions was later added to the gel as TiO_2 (anatase); F was added as dried MgF_2. The experimental procedures and conditions are as described in Della Ventura et al. (1991).

All synthesis products were examined by X-ray diffraction and optical microscopy. Selected compositions were also examined by SEM, using a Cambridge Stereoscan electron microscope equipped with a quantitative analytical EDS system. Data pertinent to synthesis conditions are given in Table 1.

* Present address: Dipartimento di Scienze Geologiche, Università di Roma III, Via Segre 2, I-00146 Roma, Italy.

0003–004X/93/0910–0980$02.00

TABLE 1. Synthesis products obtained along the $RTi_{0.6}$-$FRTi_{0.6}$ join

Sample	F (apfu)	T (°C)	P (bars)	t (h)	Synthesis products*
Rich58	0.0	900	1000	48	$amph_{ss}$
Rich59	0.4	900	1000	48	$amph_{ss}$ + pr
Rich60	0.8	900	1000	48	$amph_{ss}$ + pr + tit
Rich61	1.2	900	1000	48	$amph_{ss}$ + pr + tit
Rich62	1.6	900	1000	48	$amph_{ss}$ + pr + tit
Rich63	2.0	900	1000	48	$amph_{ss}$ + tit + rut

* $Amph_{ss}$ = amphibole solid solution; pr = priderite; tit = titanite; rut = rutile.

X-ray data measurement

Powders were ground in an alumina mortar to a grain size <2 μm and mounted in Al holders with cavities 20 × 15 × 1.0 mm. To minimize preferred orientation, the surface of the sample was carefully serrated with a razor blade in a direction parallel to the X-ray beam. Step-scan powder diffraction data were obtained with a Philips PW1710 automated diffractometer equipped with incident- and diffracted-beam Soller slits, 0.5-mm divergence and antiscatter slits, a 0.2-mm receiving slit, and a curved graphite diffracted-beam monochromator. Operating conditions were 40 kV and 40 mA, with a take-off angle of 6°. The spectra were recorded using a step interval of 0.10° 2θ, with a step counting time of 5 s. Information pertinent to data measurement is given in Table 2.

Rietveld structure refinement

The structures were refined with a PC version of the DBWS-9006 program (originally written by Wiles and Young, 1981; and modified by Sakthivel and Young, 1990), which allows the refinement of up to eight phases simultaneously. Peak shape was described by a pseudo-Voigt function with a variable percentage of Lorentzian character. The full-width at half-maximum (FWHM) was varied as a function of 2θ using the semiempirical function of Caglioti et al. (1958). Peak asymmetry and preferred orientation were corrected using the expressions of Rietveld (1969). Details and rationale for the general refinement procedure are given in Raudsepp et al. (1990). In brief, our strategy is to use accurate values for the individual isotropic displacement factors and keep them fixed during the refinement. Site occupancies can then be refined without strong correlations with the displacement factors. We refined an overall displacement factor that scales all the individual (fixed) values, but does not alter their relative values. These individual values can be derived by the inspection of single-crystal structures or by the refinement of ordered end-member amphiboles with fixed site occupancies. These values need to be adjusted to allow for disorder at intermediate compositions (see Raudsepp et al., 1990). For these potassium richterite samples, unconstrained site occupancy refinement deviated significantly from nominal occupancy for ideal end-member potassium richterite (i.e., M1 = M2 = M3 = Mg; T1 = T2 = Si) only for the T2 site, which showed significantly increased scattering over an assigned occupancy of Si. Thus all site occupancies except that of T2 were set to nominal, and the T2 occupancy was refined (together with all other variable structural and pattern parameter) as Si + Ti. Final convergence was assumed when the largest parameter shift was $<10\%$ (average $<1\%$). At that stage, we again refined the occupancies of the other sites, but these did not change significantly from nominal and so were considered to be nominal and fixed as such in the final cycles of refinement. The refined cell dimensions are given in Table 3, final atomic positions in Table 4[1], interatomic distances in Table 5[1], observed

[1] Tables 4, 5, and 6 may be ordered as Document AM-93-536 from the Business Office, Mineralogical Society of America, 1130 Seventeenth Street NW, Suite 330, Washington, DC 20036, U.S.A. Please remit $5.00 in advance for the microfiche.

TABLE 2. Data measurement and structure refinement details of Ti-rich potassium richterite samples

	Rich58	Rich59	Rich60	Rich61	Rich62	Rich63
2θ scan range (°)	9–100	9–100	9–100	9–100	9–100	9–100
Step interval (°2θ)	0.10	0.10	0.10	0.10	0.10	0.10
Integration time/step (s)	5	5	5	5	5	5
Maximum step intensity (counts)	3435	3538	3637	3155	2737	2955
No. of refined phases	1	2	3	3	3	3
No. of refined parameters	49	53	59	59	59	59
$N - P$	862	858	852	852	852	852
R_p	6.9	8.3	7.7	7.4	7.7	8.0
R_{wp}	9.5	10.7	10.5	10.2	10.3	10.6
$R_{expected}$	6.8	6.8	6.8	6.9	7.0	7.0
S (goodness of fit)	1.40	1.58	1.54	1.48	1.47	1.51
R_B	5.0	6.0	6.0	5.3	5.8	5.9
Durbin-Watson d statistic	1.32	1.33	1.24	1.32	1.21	1.24
Esd to be multiplied by:*	0.995	0.998	0.996	0.996	0.999	0.998
U	0.029	0.046	0.027	0.035	0.065	0.060
V	−0.014	−0.023	−0.007	−0.019	−0.052	−0.038
W	0.035	0.032	0.027	0.032	0.041	0.038
γ_1	0.375	0.410	0.474	0.401	0.432	0.458
γ_2	0.003	0.002	0.002	0.002	0.003	0.003

Note: $N - P$ = no. of observations (steps) − no. of least-squares parameters.
* Correction for local correlations (Bérar and Lelann, 1991).

TABLE 3. Unit-cell data for amphiboles along the $RTi_{0.6}$-$FRTi_{0.6}$ join

F (apfu)	a (Å)	b (Å)	c (Å)	β (°)	V (Å³)
0.0	10.0746(4)	18.0337(8)	5.2979(2)	104.906(3)	930.14
0.4	10.0613(4)	18.0314(9)	5.2963(3)	104.896(3)	928.56
0.8	10.0427(4)	18.0254(9)	5.2922(2)	104.875(3)	925.91
1.2	10.0262(4)	18.0194(9)	5.2871(2)	104.874(3)	923.19
1.6	10.0166(5)	18.0189(9)	5.2871(3)	104.908(3)	922.14
2.0	10.0149(5)	18.0099(10)	5.2862(3)	104.954(3)	920.49

TABLE 7. Refined site populations at the T2 site for the synthesized amphiboles

Sample	F (nominal) (apfu)	Ti at T2 (apfu)
Rich58	0.0	0.60
Rich59	0.4	0.56
Rich60	0.8	0.48
Rich61	1.2	0.40
Rich62	1.6	0.24
Rich63	2.0	0.16

and calculated step intensities in Table 6[1] and refined T2 site occupancies in Table 7.

Infrared and micro-Raman spectroscopies

Infrared spectra in the OH-stretching region were measured with a fully automated Perkin-Elmer 1760 FTIR spectrophotometer, equipped with a TGS detector and a KBr beamsplitter. Scan conditions were scan speed of 0.2 cm^{-1}/s nominal resolution of 1 cm^{-1}, and normal Beer-Norton apodization function. Samples were prepared as KBr disks, with a KBr per mineral ratio of 140/10 by weight. Details on IR sample preparation may be found in Robert et al. (1989).

Raman spectra were recorded on a monochannel Jobin-Yvon U1000 microspectrometer equipped with an Ar-ion laser, λ_o = 488 nm. The measurements were performed directly on the powdered synthetic sample (about 50 mg), placed under a 20-μm laser beam. Scan conditions were a step of 0.5 cm^{-1} and an integration time of 2 s. Two scans were averaged for each sample. The resulting uncertainty in the peak position is ±1 cm^{-1} for the sharpest bands and at least ±3 cm^{-1} for broad bands and shoulders.

RESULTS

Synthesis products

Table 1 shows the phase assemblages from the syntheses along the $RTi_{0.6}$-$FRTi_{0.6}$ join (Fig. 1) at 900 °C, 1 kbar. As the maximum solubility of Ti in potassium richterite is between 0.6 and 0.8 apfu at $T \geq 800$ °C for 1 kbar P_{H_2O} (Della Ventura et al., 1991), syntheses were carried out at 900 °C, 1 kbar, along the join $RTi_{0.6}$-$FRTi_{0.6}$, leaving the Ti content constant. For end-member $RTi_{0.6}$, a single-phase amphibole was obtained; for all other compositions, an assemblage of amphibole + priderite ± titanite ± rutile was observed. The amount of the additional Ti-bearing phase increased with an increase of F in the system at constant P and T, indicating a decrease in the solubility of Ti in the amphibole phase.

Observed, calculated, and difference X-ray diffraction patterns are shown in Figure 2 for sample Rich61 (Table 1). The two most intense peaks of priderite are indicated by arrows (see range 9–20° 2θ) and show that the amount of priderite is very small. Titanite was detected only after a careful examination of the residual pattern obtained by subtracting the reflections due to the amphibole and priderite from the whole powder pattern. Its presence was confirmed by SEM examination of the synthesis products.

Unit-cell dimensions

Unit-cell dimensions (Table 3) are shown in Figure 3 as a function of nominal F content of the amphibole. The a, b, and c dimensions decrease regularly along the join, whereas the β angle shows a very curious dependency on F content. There are two simultaneous changes along this series: the increase in F, and the decrease of Ti in the amphibole; both factors have been independently quantified in previous studies.

1. In Ti-free richterite and potassium richterite, the substitution of F for OH notably decreases a but has no effect on b and c (Robert et al., 1989). This strong anisotropy in the variation of the cell dimensions is common in amphiboles and micas, in which the OH group is directed perpendicular to a ring of silicate tetrahedra and faces an alkali cation at the A site. The decrease in the a dimension may be related to the suppression of the H^+-A^+ repulsion, with a consequent contraction of the structure along [100] in amphiboles (Robert et al., 1989) and [001] in trioctahedral micas (Noda and Roy, 1956; Noda and Ushio, 1966; Robert et al., 1993). For synthetic potassium richterite, there is a decrease of 0.070 Å in a when OH is completely replaced by F (Robert et al., 1989).

2. In F-free synthetic potassium richterite, the substitution of Ti for Si in the tetrahedral rings affects all cell dimensions, which increase with increasing Ti. For Ti contents ranging from 0.2 to 0.6 apfu, a increases by 0.018 Å, b increases by 0.030 Å, and c increases by 0.013 Å (Della Ventura et al., 1991).

Considering these data, we can quantify the effect of each of these two factors (F and Ti) on the individual cell dimensions as follows: (1) The a edge: the total decrease of 0.060 Å for a (Table 4) seems too low compared with what is expected when adding the effect of F replacing OH (0.070 Å) to the effect of decreasing Ti (0.018 Å). Therefore, the strong decrease of a in the present case is related only to the OH-F exchange. The trend for a seems to flatten out at very high F content (Fig. 3). Note that these amphiboles were synthesized hydrothermally, and thus the amphibole with nominal anion composition F = 2 apfu certainly contains minor quantities of OH, as also shown by FTIR (see below). This can account for the deviation from linearity observed for a in Figure 3 and V in Figure 4. (2) The b edge: a decrease of 0.033 Å is

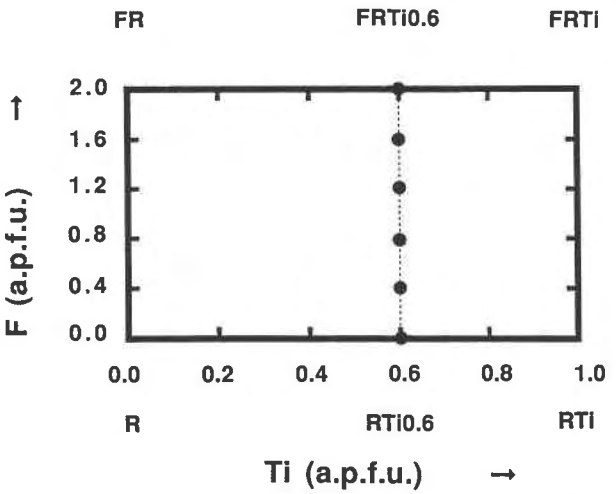

Fig. 1. Schematic diagram showing the investigated system. The broken line represents the experimental join; dots represent the starting compositions. R = $K(NaCa)Mg_5Si_8O_{22}(OH)_2$; $RTi_{0.6}$ = $K(NaCa)Mg_5[Si_{7.4}Ti_{0.6}]O_{22}(OH)_2$; RTi = $K(NaCa)Mg_5[Si_7Ti_1]O_{22}(OH)_2$; FR = $K(NaCa)Mg_5Si_8O_{22}(F)_2$; $FRTi_{0.6}$ = $K(NaCa)Mg_5[Si_{7.4}Ti_{0.6}]O_{22}(F)_2$; FRTi = $K(NaCa)Mg_5[Si_7Ti_1]O_{22}(F)_2$.

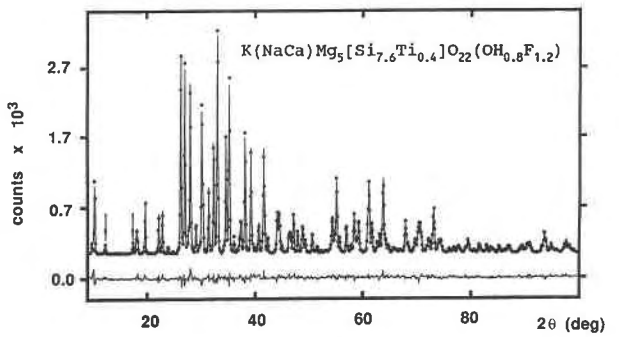

Fig. 2. Observed (solid line), calculated (dots), and difference (bottom solid line) powder diffraction patterns for the product corresponding to the starting composition 40% $RTi_{0.6}$ 60% $FRTi_{0.6}$. The arrows indicate the two most intense reflections of priderite.

observed here, in close agreement with the value measured for F-free Ti-bearing richterite with a Ti content decreasing from 0.6 to 0.2 apfu. Thus the decrease in b is completely due to the effect of decreasing Ti in these amphiboles (0.030 Å). (3) The c edge: again the decrease of c observed here (0.015 Å, Table 4) is in close agreement with that expected if one considers only the effect of Ti in these amphiboles (0.013 Å).

Thus the effect of the OH-F substitution in Ti-rich richterite is the same as that observed in Ti-free richterite.

It is unclear whether the unusual variation observed for β is significant, but it can be explained by taking into account the contrasting effects of the reduction in size of the octahedral strip and the tetrahedral double chain. For a F content in the range 0.0–1.0 apfu, the decrease in size of the octahedral strip is dominant, and a decrease of the β angle is observed. Because of the significant decrease of $^{[4]}$Ti for F > 1.0 apfu, shrinkage of the tetrahedral units becomes predominant, and an increase of the displacement between the chains is required to ensure the fit between the structural units. On the other hand, the variation in β is very small; the above argument seems reasonable, but it is difficult to find it convincing in view of the small variations involved.

Bond lengths

For the Ti-rich richterite samples synthesized here, ⟨T1-O⟩ is constant at ≃1.600 Å, whereas ⟨T2-O⟩ decreases from 1.645 to 1.635 Å across the series. Both ⟨T-O⟩ distances are somewhat shorter than those measured by single-crystal diffractometry on natural samples of similar compositions (Oberti et al., 1992). However, it is noteworthy that ⟨T2-O⟩ decreases regularly with decreasing $^{[4]}$Ti, in agreement with what has been observed by X-ray single-crystal diffraction (Oberti et al., 1992).

According to Oberti et al. (1992), changes in anion occupancy at O(3) affect the dimensions of the M1 and M3 octahedra. Thus a linear decrease in size of the grand ⟨M-O⟩ lengths is to be expected along the join, provided that no changes occur in the cation occupancies over the M octahedra. The linear trend shown in Figure 5 indicates that this is the case for our synthetic hydroxyl fluorine richterite samples.

Site occupancies

The site-scattering refinements show that Ti is completely ordered at T2. Only the OH end-member is stable, with a Ti content equal to the maximum allowed for the experimental conditions used here (Table 7). With increasing F content, the amount of Ti in the amphibole decreases from 0.60 to 0.16 apfu (Table 7). This accounts for the parallel increase in the amount of Ti-bearing accessory phases in the synthesis products.

The variation of ⟨M-O⟩ (Fig. 5) is related only to the linear decrease of F, indicating that no changes occur in the occupancies of the M sites. We can rule out the occurrence of Ti^{4+} at M1 (where it has been found in some $^{[6]}$Ti-bearing richterite samples refined by Oberti et al., 1992) anywhere along the join. This would have been recorded by an increase in M1 scattering and a decrease of ⟨M-O⟩, neither of which occurs in these amphiboles.

Infrared spectroscopy

The FTIR spectra of our synthetic amphiboles in the OH-stretching region (3800–3600 cm^{-1}) are shown in Figure 6. The disks were prepared using the bulk powder, but the additional phases present are minor and anhydrous, and the bands observed in this region are due only to amphibole.

In the $RTi_{0.6}$ end-member, there is a single asymmetric band at 3728 cm^{-1} and a minor band at 3670 cm^{-1}. The main band at 3728 cm^{-1} is assigned to OH dipoles facing occupied A sites and directly coordinated by three Mg

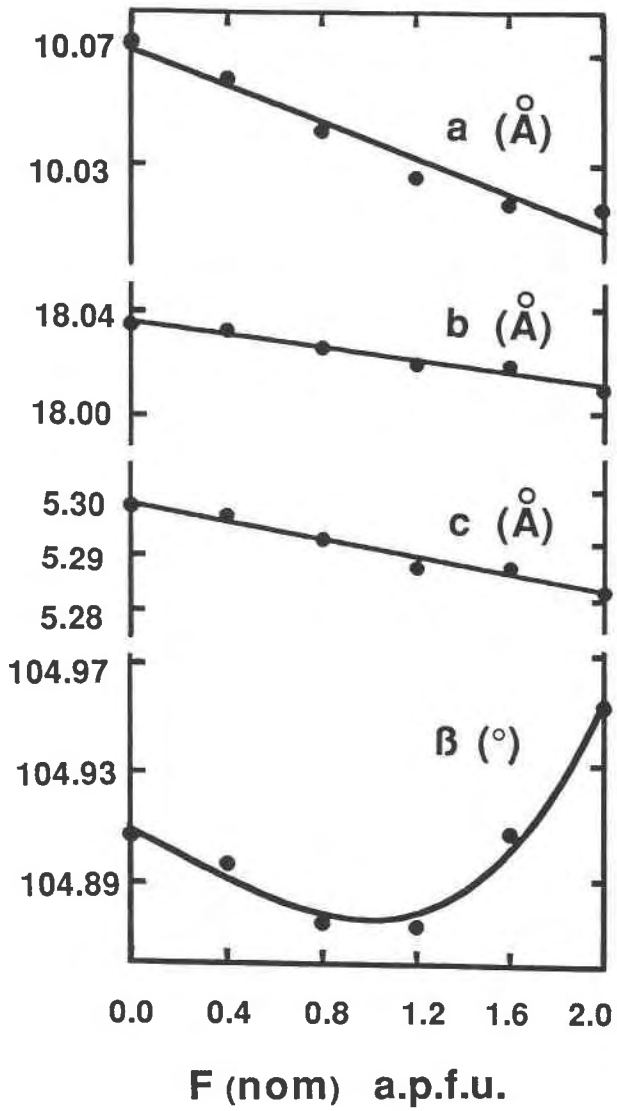

Fig. 3. Variation of the unit-cell dimensions for amphiboles along the $RTi_{0.6}$-$FRTi_{0.6}$ join as a function of the nominal F content.

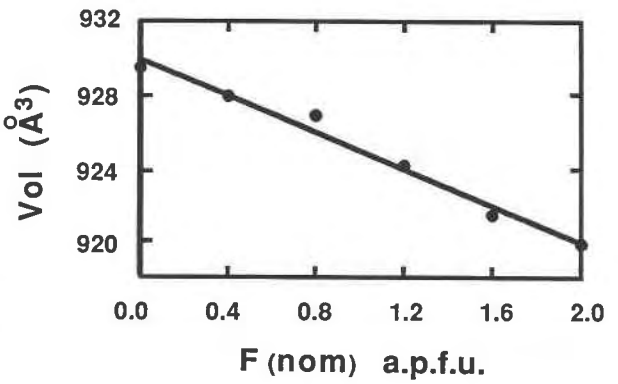

Fig. 4. Variation of the cell volume for amphiboles along the $RTi_{0.6}$-$FRTi_{0.6}$ join as a function of the nominal F content.

cations (Rowbotham and Farmer, 1973; Robert et al., 1989; Della Ventura and Robert, 1990; Della Ventura et al., 1991). The assignment of the minor band at 3670 cm^{-1} is more difficult. This band is ubiquitous in both natural and synthetic richterite, and its frequency corresponds to the principal band in tremolite. The band was originally assigned to vacant A site configurations in richterite, i.e., solid solutions toward tremolite (Rowbotham and Farmer, 1973), but there are difficulties with this assignment (Robert et al., 1989; Della Ventura and Robert, 1990). There is good evidence to indicate that it is not due to an empty A site configuration in richterite (Della Ventura et al., 1991); but an adequate assignment has yet to be proposed. However, one thing is certain: it is present in Ti-free synthetic richterite and potassium richterite (Rowbotham and Farmer, 1973; Robert et al., 1989) and hence cannot be assigned to configurations involving Ti at M1 or M3.

There are no data available for the OH-stretching wavenumbers of an OH group linked to an Mg_2Ti cluster in amphiboles. However, an example is known for trioctahedral micas: in Ti-rich phlogopite, where OH is bonded to Mg_2Ti (Robert, unpublished data), the principal OH-stretching frequency of this local configuration is below 3660 cm^{-1}. No bands are observed in this range in our Ti-rich richterite samples, indicating that there is no significant Ti occupying M1 or M3 when O3 is occupied by OH. However, if Ti were to occur at M1 or M3 coupled with the replacement of OH^- by O^{-2} at both neighboring O3 positions by means of the substitution $^{M1,M3}Ti^{4+} + 2^{O3}O^{2-} \rightleftharpoons {}^{M1,M3}Mg + 2^{O3}OH^-$ (Oberti et al., 1992); this configuration would be invisible to infrared spectroscopy in the OH-stretching region. The occurrence of Ti at M2 would not result in an additional OH band in the infrared, although possibly it would produce some substitutional broadening. Hence these two possibilities cannot be discounted on the basis of the infrared spectra in the OH region. However, the Rietveld results show that the octahedral sites are occupied only by Mg, conformable with the lack of OH bands that can be assigned to local configurations involving Ti. The complementary XAS (X-ray Absorption Spectroscopy) results (Mottana et al., 1990; Paris et al., 1993) from these samples are in agreement with the occurrence of Ti only in tetrahedral coordination in these synthetic amphiboles.

Along the $RTi_{0.6}$-$FRTi_{0.6}$ join (Fig. 6), the main OH-stretching band gradually decreases in intensity and finally becomes unobservable, while a new band centered at 3711 cm^{-1} becomes more intense with increasing F content; the position of this new band is constant across the series. Solid solution series involving (OH,F) substitution are common in minerals, and two types of behavior are observed with respect to their infrared spectra in the OH-stretching region. In some series (e.g., amblygonite-montebrasite: Fransolet and Tarte, 1977; Groat et al., 1990; trioctahedral micas: Robert et al., 1993); only

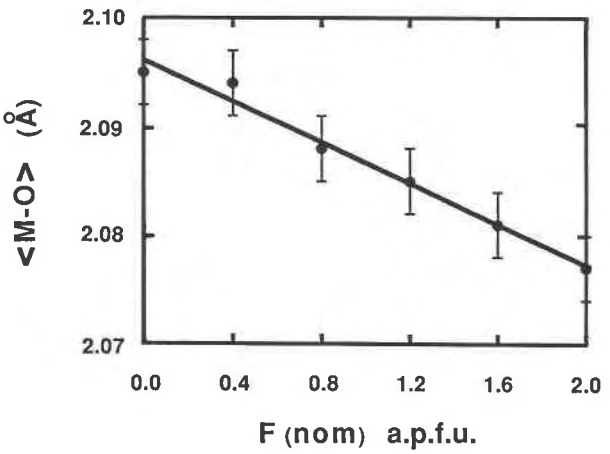

Fig. 5. Variation of the grand ⟨M-O⟩ bond lengths for amphiboles along the $RTi_{0.6}$-$FRTi_{0.6}$ join as a function of the nominal F content.

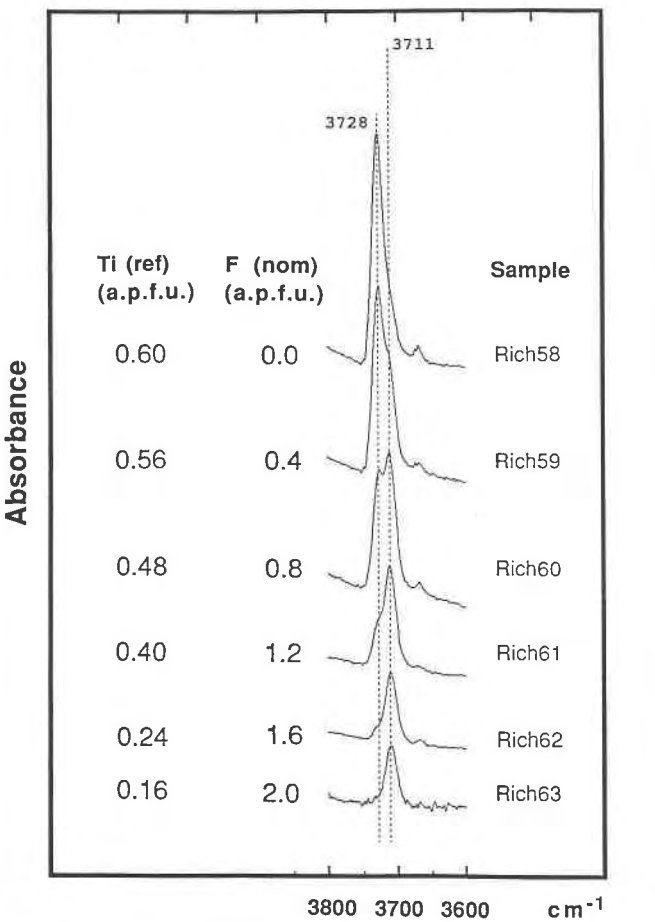

Fig. 6. IR spectra of Ti-rich potassium richterite in the OH-stretching region.

one single absorption band is observed. With varying composition, this band gradually shifts in wavenumber and may broaden; however, no well-resolved hyperfine structure is observed. This suggests an essentially random distribution of OH and F in these structures. In other series (e.g., richterite and potassium richterite, Robert et al., 1989), partial substitution of OH by F is accompanied by the appearance of one additional band at a lower wavenumber. This is also the case for the Ti-bearing richterite samples investigated here. This fact suggests that the local OH-F distribution is not random in these amphiboles.

Inspection of Figure 6 shows that the principal band in the F-free sample is markedly asymmetric, suggesting the presence of a weak component at ~3711 cm^{-1}. This cannot be due to a local configuration involving F (i.e., F-MgMgMg-OH), as this sample is F-free. However, Della Ventura et al. (1991) have shown that there is a weak band in the spectrum of (F-free) Ti-bearing potassium richterite, the intensity of which increases with increasing Ti content. The only possible origin for this band involves OH-MgMgMg-OH configurations with Ti at T2 in the next-nearest-neighbor position; this accounts for the small shift in frequency from the normal OH-MgMgMg-OH band, and for the weak intensity. As F increases (Fig. 6), Ti decreases and the intensity of this weak band will decrease even further. There is an accidental overlap with the F-MgMgMg-OH band in the F-bearing samples, and so this weak peak is only apparent when F-MgMgMg-OH configurations are absent (i.e., in the F-free sample).

Raman scattering

In the range 1200–600 cm^{-1}, the spectra (Fig. 7) are similar to those recorded for F-free titanium richterite; detailed band-assignments are discussed by Della Ventura et al. (1991). The sharp, intense band at 681 cm^{-1} is assigned to the symmetric Si-O-Si vibration; its wavenumber is constant across the series and is not affected by the OH-F substitution. The Raman spectra show vibrations typical of $^{[4]}Ti^{4+}$: the sharp band at 897 cm^{-1}, the 926 cm^{-1} shoulder, the broad bands around 853, 835, and 778 cm^{-1} (Fig. 7). With increasing F (and decreasing Ti) content in the amphibole, the most notable feature is the regular decrease in intensity of the groups of overlapping bands in the range 930–800 cm^{-1} and, in particular, the most prominent band at 897 cm^{-1}. This feature, combined with the Rietveld results, supports the previous assignment of these bands to $Ti^{4+}O_4$ vibrations (Della Ventura et al., 1991). All other bands (1200–1000 cm^{-1}) are assigned to antisymmetric SiO_4 vibrations, there is no significant change in frequency of these bands across the series. In particular, the constant frequency and intensity of the band at 1070 cm^{-1}, assigned to the vibration of the $T1O_4$ group, is consistent with the fact that the T1 tetrahedron is not involved in the Si-Ti substitution (Oberti et al., 1992).

In the region 600–30 cm^{-1}, bands due to distortion of the tetrahedral chains and to M-O and A-O stretching vibrations occur. New bands appear in this region at relatively constant wavenumbers. These bands, not present

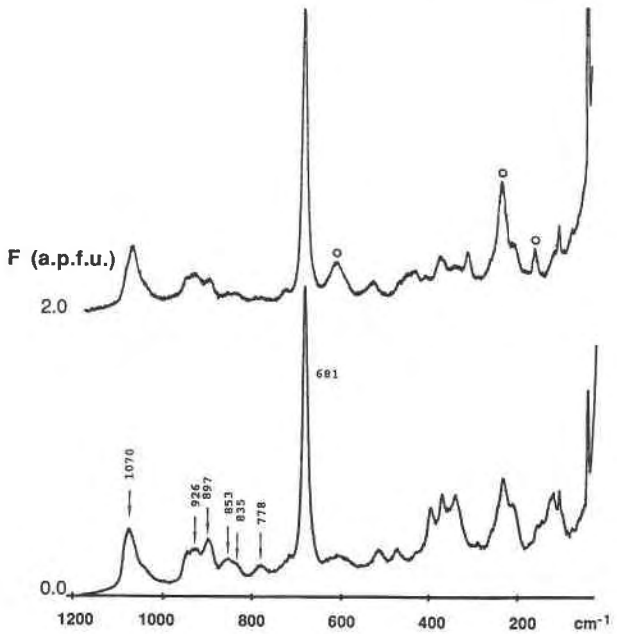

Fig. 7. Raman spectra in the region 1200–30 cm^{-1} for the end-member synthesis products as a function of F (and Ti) contents. Arrows = bands typical of [4]Ti-O groups. Open circles = bands typical of rutile.

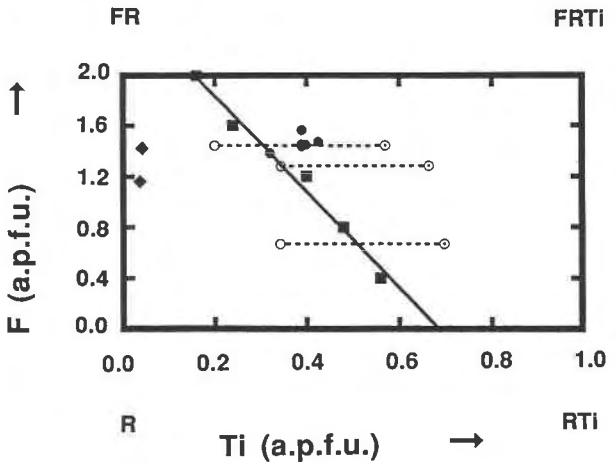

Fig. 8. Schematic representation of the stability field of Ti-rich potassium richterite. Solid squares = this work. All other data are natural richterite (Oberti et al., 1992): open circles with point = samples containing both [4]Ti and [6]Ti; open circles = same samples with Ti assigned to T2; solid circles = samples with high [4]Ti and coexisting with Ti-bearing phases; solid diamonds = samples containing low Ti and not coexisting with Ti-bearing phases.

in the spectrum of the F-free end-member, are assigned to the additional Ti-bearing phases that occur in the synthesis products with increasing F content. In particular, the bands at 610, 240, and 150 cm^{-1} correspond closely to those observed in rutile; they are indicated by open circles in Figure 7.

Discussion

This study provides direct evidence for the tetrahedral coordination of Ti^{4+} in synthetic richterite. Refinement of site occupancies shows that the amount of [4]Ti in these synthetic amphiboles decreases rapidly with increasing F in the solid-solution series (Fig. 8). The points representing the refined Ti at T2 as a function of the nominal F content define a well-developed linear trend. This marks the upper limit of the [4]Ti solubility in potassium richterite as a function of F at high temperatures and low P_{H_2O} (the most favorable conditions for Ti incorporation in richterite: Della Ventura et al., 1991).

The intercept along the R-RTi join is at 0.7 Ti apfu. This value should be considered as the maximum Ti content in Fe-free richterite at 1 kbar. It is in close agreement with previous experimental data and with all data reported from natural occurrences (Wagner and Velde, 1986; Thy et al., 1987). Most analyses of Ti-rich richterite (from lamproites) do not include data for F. However, some data are available in Oberti et al. (1992), shown in Figure 8. These data are from richterite coexisting with Ti-rich phases, which ensures that these amphiboles contain the maximum possible amount of Ti allowed by their conditions of crystallization. There are three samples (circled dots in Fig. 8) which lie significantly outside the stability field of Ti-rich richterite determined in the present study, apparently having an excess of Ti. However, Oberti et al. (1992) show that a significant amount of Ti in these amphiboles is not tetrahedrally coordinated but is octahedrally coordinated, entering the structure by means of an oxy-substitution of the form $^{M1}Mg^{2+} + 2^{O3}(OH,F)^{-} = {}^{M1}Ti^{4+} + 2^{O3}O^{2-}$. If [4]Ti only is plotted instead of Ti_{tot} for the natural samples of Figure 8 (open circles), the three errant samples fall within the stability field defined by the present experimental study.

Some other analyses for which the F contents are known exceed the solubility limit of Ti defined here. All these samples contain appreciable amounts of Fe^{2+} (Oberti et al., 1992). There is strong evidence for the favorable effect of Fe on the solubility of Ti in ferromagnesian micas (Czamanske and Wones, 1973; Abrecht and Hewitt, 1988), but until now no data were available for amphiboles. Figure 8 suggests that Fe^{2+} increases the solubility limit of Ti for amphiboles as well. However, this needs to be experimentally verified, and such a study is currently under way.

The [4]Ti usually prefers silicates with isolated tetrahedra. As noted by Della Ventura et al. (1991), potassium richterite is the first example of a polymerized silicate containing [4]Ti as a major constituent. It is noteworthy that with the two types of tetrahedra present in the amphibole structure, T1 with three bridging O atoms and T2 with only two, [4]Ti is not randomly distributed over these sites. It is completely ordered at T2, the tetrahedron with the lower number of bridging O atoms. Note that

this contrasts with the behavior of Ti in kaersutite (Kitamura et al., 1975; Hawthorne and Grundy, 1973; Waychunas, 1987), in which Ti is octahedrally coordinated.

A crystal-chemical explanation for the ordering of Ti^{4+} at T2 has been proposed by Oberti et al. (1992). In richteritic amphiboles, the dimension of the octahedral layer is the largest possible for an amphibole with its A site filled; therefore, tetrahedral substitutions with cations larger than Si^{4+} are favored. The preference of Ti^{4+} for T2 is a consequence of stereochemical and local charge-balance requirements. Furthermore, the temperature dependence of the solubility of $^{[4]}Ti^{4+}$ in richterite, may be explained by taking into account the larger thermal expansion coefficients of the octahedral strip compared with that of the tetrahedral chain (Oberti et al., 1992). As a consequence of this fact, the $Ti^{4+} \rightleftharpoons Si$ substitution is favored at high temperatures. On the basis of this model, we can also explain the decrease of solubility of $^{[4]}Ti^{4+}$ with increasing F content: the overall reduction in size of the octahedral strip with increasing F content requires a parallel reduction in size of the tetrahedral chains (achieved by excluding Ti from the T2 site) in order to ensure a fit between the two structural units. This model also provides an explanation for the favorable effect of Fe^{2+} on the increase of solubility of $^{[4]}Ti^{4+}$ in richterite: the substitution of Fe^{2+} for Mg at the M1, M2, and M3 sites enlarges the octahedral strip, thus favoring substitution of the larger Ti^{4+} for Si in the tetrahedral chains.

Acknowledgments

Part of the work was done during the stay of G.D.V. at the Department of Geological Sciences, University of Manitoba, supported by an International Council for Canadian Studies grant. Financial assistance was provided by a CNR grant 92-00774-CT05 to G.D.V. and by Natural Sciences and Engineering Research Council of Canada Operating, Infrastructure, and Major Equipment grants to F.C.H. The final draft of the paper benefited from the constructive criticism and suggestions of A. Hofmeister, A. Mottana, R. Oberti, J. Post, and L. Ungaretti, to all of whom sincere thanks are due.

References cited

Abrecht, J., and Hewitt, D.A. (1988) Experimental evidence on the substitution of Ti in biotite. American Mineralogist, 73, 1275–1284.

Bérar, J.-F., and Lelann, P. (1991) E.S.D.'s and estimated probable error obtained in Rietveld refinements with local correlations. Journal of Applied Crystallography, 24, 1–5.

Caglioti, G., Paoletti, A., and Ricci, F.P. (1958) Choice of collimators for a crystal spectrometer for neutron diffraction. Nuclear Instruments, 3, 223–228.

Czamanske, G.K., and Wones, D.R. (1973) Oxidation during magmatic differentiation, Finnmarka complex, Oslo area, Norway. II. The mafic silicates. Journal of Petrology, 14, 349–380.

Della Ventura, G., and Robert, J.-L. (1988) OH-stretching region IR study of Ti-rich synthetic richterites (abs.). Terra Cognita, 8, 60.

——— (1990) Synthesis, XRD and FTIR studies of strontium richterites. European Journal of Mineralogy, 2, 171–175.

Della Ventura, G., Robert, J.-L., and Bény, J.-M. (1991) Tetrahedrally coordinated Ti^{4+} in synthetic Ti-rich potassic richterites: Evidence from XRD, FTIR, and Raman studies. American Mineralogist, 76, 1134–1140.

Fransolet, A.-M., and Tarte, P. (1977) Infrared spectra of analyzed samples of the amblygonite-montebrasite series: A new rapid semi-quantitative determination of fluorine. American Mineralogist, 62, 559–564.

Groat, L.A., Raudsepp, M., Hawthorne, F.C., Ercit, T.S., Sheriff, B.L., and Hartman, J.S. (1990) The amblygonite-montebrasite series: Characterization by single-crystal structure refinement, infrared spectroscopy, and multinuclear MAS-NMR spectroscopy. American Mineralogist, 75, 992–1008.

Hamilton, D.L., and Henderson, C.M.B. (1968) The preparation of silicate compositions by a gelling method. Mineralogical Magazine, 36, 832–838.

Hawthorne, F.C., and Grundy, H.D. (1973) The crystal chemistry of the amphiboles. II. Refinement of the crystal structure of oxy-kaersutite. Mineralogical Magazine, 39, 390–400.

Kitamura, M., Tokonami, M., and Morimoto, N. (1975) Distribution of titanium atoms in oxy-kaersutite. Contributions to Mineralogy and Petrology, 51, 167–172.

Mottana, A., Paris, E., Della Ventura, G., and Robert, J.-L. (1990) Spectroscopic evidence for tetrahedrally-coordinated titanium in richteritic amphiboles. Rendiconti Fisici Accademia Lincei, 9 (1), 387–392.

Noda, T., and Roy, R. (1956) OH-F exchange in fluorine phlogopite. American Mineralogist, 41, 929–932.

Noda, T., and Ushio, M. (1966) Hydrothermal synthesis of fluorine hydroxyphlogopite. II. Relationship between the fluorine content, lattice constants and the conditions of synthesis of fluorine-hydroxy-phlogopite. Collected Papers, Synthetic Crystal Research Laboratory, Faculty of Engineering, Nagoya University, Japan, 3, 96–104.

Oberti, R., Ungaretti, L., Cannillo, E., and Hawthorne, F.C. (1992) The behaviour of Ti in amphiboles. I. Four- and six-coordinated Ti in richterite. European Journal of Mineralogy, 4, 425–439.

Paris, E., Mottana, A., Della Ventura, G., and Robert, J.-L. (1993) Titanium valence and coordination in synthetic richterite–Ti-richterite amphiboles: A synchrotron-radiation XAS study. European Journal of Mineralogy, 5, 455–464.

Raudsepp, M., Hawthorne, F.C., and Turnock, A.C. (1990) Crystal chemistry of synthetic pyroxenes on the join $CaNiSi_2O_6$-$CaMgSi_2O_6$ (diopside): A Rietveld structure refinement study. American Mineralogist, 75, 1274–1281.

Rietveld, H.M. (1969) A profile refinement method for nuclear and magnetic structures. Journal of Applied Crystallography, 2, 65–71.

Robert, J.-L., Della Ventura, G., and Thauvin, J.-L. (1989) The infrared OH-stretching region of synthetic richterites in the system Na_2O-K_2O-CaO-MgO-SiO_2-H_2O-HF. European Journal of Mineralogy, 1, 203–211.

Robert, J.-L., Bény, J.-M., Della Ventura, G., and Hardy, M. (1993) Fluorine in micas. Crystal-chemical control of the OH-F distribution between trioctahedral and dioctahedral sites. European Journal of Mineralogy, 5, 7–18.

Rowbotham, G., and Farmer, V.C. (1973) The effect of "A" site occupancy on the hydroxyl stretching frequency in clinoamphiboles. Contributions to Mineralogy and Petrology, 38, 147–149.

Sakthivel, A., and Young, R.A. (1990) Programs DBWS-9006 and DBWS-9006PC for Rietveld analysis of X-ray and neutron powder diffraction patterns. Georgia Institute of Technology, Atlanta, Georgia 30332, U.S.A.

Thy, P., Stecher, O., and Korstgard, J.A. (1987) Mineral chemistry and crystallization sequences in kimberlite and lamproite dikes from the Sisimiut area, central West Greenland. Lithos, 20, 391–417.

Wagner, C., and Velde, D. (1986) The mineralogy of K-richterite bearing lamproites. American Mineralogist, 71, 17–37.

Waychunas, G. (1987) Synchrotron radiation XANES spectroscopy of Ti in minerals: Effect of Ti bonding distances, Ti valence and site geometry on absorption edge structure. American Mineralogist, 72, 89–101.

Wiles, D.B., and Young, R.A. (1981) A new computer program for Rietveld analysis of X-ray powder diffraction patterns. Georgia Institute of Technology, Atlanta, Georgia 30332, U.S.A.

Manuscript received February 12, 1992
Manuscript accepted April 25, 1993